Cell Reports
Report

Epigenetic Reprogramming of Human Embryonic Stem Cells into Skeletal Muscle Cells and Generation of Contractile Myospheres

Sonia Albini,[1] Paula Coutinho,[1] Barbora Malecova,[1] Lorenzo Giordani,[1] Alex Savchenko,[1] Sonia Vanina Forcales,[1,3] and Pier Lorenzo Puri[1,2,*]
[1]Sanford-Burnham Institute for Medical Research, La Jolla, CA 92037, USA
[2]IRCCS Fondazione Santa Lucia, Rome 00143, Italy
[3]Present address: Institute of Predictive and Personalized Medicine of Cancer (IMPPC), Badalona, Spain
*Correspondence: lpuri@sanfordburnham.org
http://dx.doi.org/10.1016/j.celrep.2013.02.012

SUMMARY

Direct generation of a homogeneous population of skeletal myoblasts from human embryonic stem cells (hESCs) and formation of three-dimensional contractile structures for disease modeling in vitro are current challenges in regenerative medicine. Previous studies reported on the generation of myoblasts from ESC-derived embryoid bodies (EB), but not from undifferentiated ESCs, indicating the requirement for mesodermal transition to promote skeletal myogenesis. Here, we show that selective absence of the SWI/SNF component BAF60C (encoded by *SMARCD3*) confers on hESCs resistance to MyoD-mediated activation of skeletal myogenesis. Forced expression of BAF60C enables MyoD to directly activate skeletal myogenesis in hESCs by instructing MyoD positioning and allowing chromatin remodeling at target genes. BAF60C/MyoD-expressing hESCs are epigenetically committed myogenic progenitors, which bypass the mesodermal requirement and, when cultured as floating clusters, give rise to contractile three-dimensional myospheres composed of skeletal myotubes. These results identify BAF60C as a key epigenetic determinant of hESC commitment to the myogenic lineage and establish the molecular basis for the generation of hESC-derived myospheres exploitable for "disease in a dish" models of muscular physiology and dysfunction.

INTRODUCTION

Generation of tridimensional (3D) structures that recapitulate histological and functional properties of adult organs and tissues is a current challenge in regenerative medicine because it requires abundant and homogeneous population of committed progenitors from human embryonic stem cells (hESCs). For instance, formation of hESC-derived contractile 3D skeletal muscles has never been reported, reflecting the unsuccessful attempts to directly generate homogeneous populations of skeletal muscle progenitors from undifferentiated hESCs. Previous studies have demonstrated that generation of skeletal myoblasts could be achieved from embryoid body (EB)-derived mesodermal cells (Darabi et al., 2008, 2012; Iacovino et al., 2011) or from mesenchymal derivatives of ESCs (Barberi et al., 2007; Goudenege et al., 2012), indicating the requirement for transition through the mesodermal stage to activate skeletal myogenesis. This evidence suggests an "intrinsic" resistance to the activation of the myogenic program in ESCs prior to mesoderm formation. Indeed, no evidence of direct generation of skeletal muscle progenitors from undifferentiated hESCs has been reported so far, raising the question of whether hESCs can be directly reprogrammed into skeletal muscle cells. Direct myogenic conversion of somatic nonmuscle cells upon introduction of MyoD has provided evidence that a single tissue-specific transcriptional activator is able to reprogram the nucleus of host cells into the skeletal muscle phenotype (Weintraub et al., 1989; Gerber et al., 1997; Chambers and Studer, 2011). However, it is currently unknown whether ESCs can be reprogrammed into skeletal myoblasts by ectopic expression of MyoD.

RESULTS AND DISCUSSION

Selective Absence of BAF60C in hESCs Prevents Activation of Skeletal Myogenesis by Ectopic Expression of MyoD

We tested the ability of hESCs to undergo direct myogenic conversion in response to the ectopic expression of MyoD as compared to human fibroblasts that typically convert into skeletal muscle cells upon MyoD expression (Weintraub et al., 1989). Surprisingly, expression of MyoD in hESCs failed to activate skeletal myogenesis under the same culture conditions in which massive myogenic conversion was observed upon expression of MyoD in H27 human fibroblasts (Figure 1A and Figure S1A). Resistance to MyoD-induced myogenic conversion was observed in different hESC lines tested (H9 and H1) (Figure S1B). Figure 1A shows that ectopic MyoD was expressed at comparable levels and was properly localized in the nuclei of hESCs as well as fibroblasts but failed to activate muscle gene expression only in hESCs (Figure 1A and Figure S1),

Cell PRESS
Open ACCESS

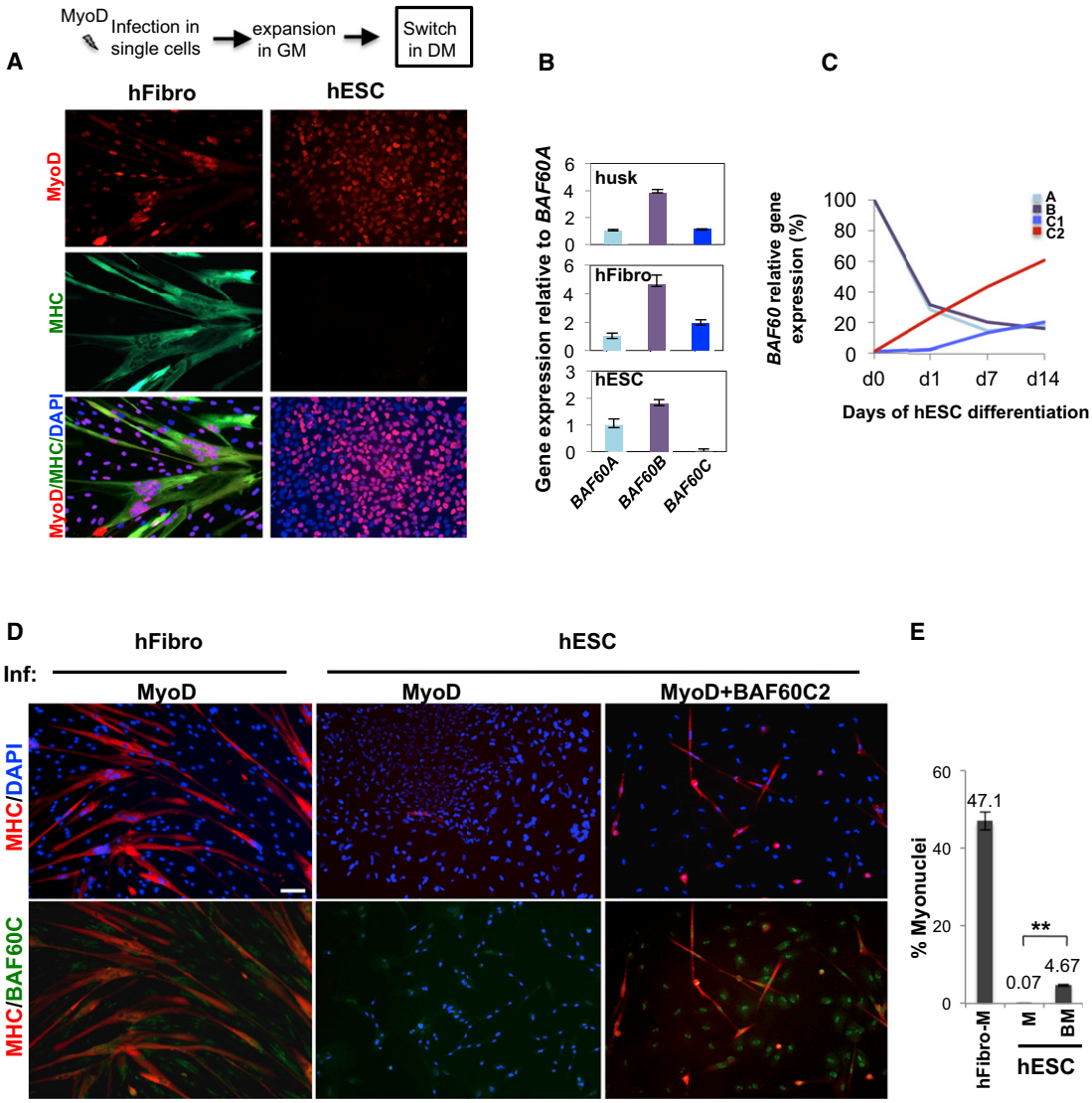

Figure 1. BAF60C2 Rescues MyoD-Mediated Myogenic Conversion in hESCs

(A) Immunofluorescence staining to detect myosin heavy chain (MHC) (green) and MyoD (red) in human fibroblasts (H27) and hESCs (H9) infected with MyoD or a control virus (Pgk). Nuclei are visualized by DAPI staining (blue). Cells were cultured in monolayer and induced to differentiate by shifting medium from growing conditions (growth medium [GM]) to promyogenic differentiation medium (DM). See Experimental Procedures for details.

(B) Relative gene expression of BAF60 subunits (A,B,C) in hESCs (H9), human skeletal myoblasts (husk), and human fibroblasts (H27). Error bars represent ±SD.

(C) Relative gene expression of BAF60 variants and human BAF60C isoforms C1 and C2 were measured at the indicated time points during H9 differentiation into EBs.

(D) Representative fluorescence staining to detect MHC (red) and Baf60c (green) in human fibroblasts (H27) infected with lentivirus expressing MyoD and in hESCs (H9) with lentiviruses expressing MyoD alone or together with BAF60C2. After infection, cells were cultured in monolayer and induced to differentiate by shifting medium from GM to DM.

(E) Efficiency of myogenic conversion was calculated as a percentage of the nuclei contained within the myotubes (n = 3; error bars represent ±SD).

See also Figures S1and S2.

suggesting that hESCs might have a "nuclear landscape" not permissive for activation of the myogenic program. We reasoned that this could be due to a deficiency in a key component(s) of the chromatin-modifying machinery that enables MyoD to activate transcription from target genes. We therefore analyzed the integrity of the chromatin-modifying complexes that are known to enable MyoD-activated gene expression (de la Serna et al., 2006; Guasconi and Puri, 2009; Sartorelli and Juan, 2011). We measured by quantitative RT-PCR (qRT-PCR) the expression levels of key components of these complexes in distinct hESC lines (H1, H7, and H9) and human H27 fibroblasts and found that the large majority of them were expressed in all cell lines analyzed, with the notable exception of the structural subunits of the SWI/SNF chromatin remodeling complex, *BAF60C*

(encoded by *SMARCD3)*, and the alternative SWI/SNF ATPase *BRM* (Figure S2). Lack of Baf60c and Brm proteins in mouse embryonic stem cells was previously observed by Crabtree and colleagues (Ho et al., 2009). However, while Baf60c is absolutely required for the activation of skeletal myogenesis (Forcales et al., 2012; Lickert et al., 2004), Brm appears dispensable (Reyes et al., 1998), with Brg1 being the essential ATPase of the SWI/SNF complex that remodels the chromatin at MyoD target genes (Ohkawa et al., 2006; Forcales et al., 2012). Three alternative variants of the BAF60 subunits—BAF60A, B, and C—are expressed in somatic cells, with mutually exclusive presence in distinct SWI/SNF complexes (Debril et al., 2004; Wang et al., 1996). Of note, while all three variants are expressed in human skeletal myoblasts and fibroblasts, which are competent to activate the myogenic program, expression of *BAF60A* and *B,* but not *BAF60C,* was detected in hESCs, which are resistant to the activation of the myogenic program (Figure 1B). Interestingly, *BAF60C* was induced upon EB formation (Figure 1C), a stage permissive for the activation of skeletal myogenesis (Iacovino et al., 2011). Two *BAF60C* isoforms are expressed in human somatic cells: *BAF60C1* and *BAF60C2.* However, only *BAF60C2* was significantly upregulated during EB formation (Figure 1C). Thus, we hypothesized that BAF60C2 could be a limiting factor for the direct activation of the myogenic program in hESCs and tested whether forced expression of BAF60C2 in hESCs could restore MyoD-mediated activation of the myogenic program. Figures 1D and 1E show that ectopic expression of BAF60C2 enabled MyoD-directed conversion of hESCs into myosin heavy chain (MyHC)-positive muscle cells.

Efficient Generation of Skeletal Muscle Cells from hESCs Requires an Epigenetic Commitment by BAF60C2 and MyoD, Followed by Activation of Skeletal Myogenesis within Floating Clusters

Because the efficiency of myogenic conversion in BAF60C2/MyoD-expressing hESCs was reduced as compared to the myogenic conversion of MyoD-expressing fibroblasts (Figure 1E), we considered the possibility that hESCs could receive optimal differentiation cues from their physiological context; that is, the network of signals generated by cell aggregation (such that occurring within EBs) (Keller, 1995). It is well established that cell-to-cell interactions promote intracellular promyogenic signaling (Krauss, 2010). To this purpose, we devised a protocol for generation of skeletal muscle cells from hESCs that included the transition through an aggregation stage (EB-like clusters) equivalent to the standard culture conditions that typically promote EBs from hESCs (see scheme in Figure 2A and Experimental Procedures for details). We generated hESCs (H9 line) stably expressing BAF60C2 and MyoD (hereby referred to as $hESC^{BAF60C2/MyoD}$) and cultured them in conditions permissive for aggregation into floating clusters for 5 days (pre-EB conditions), followed by dissociation into single cells that were subsequently exposed to standard myogenic differentiation medium (post-EB condition; see scheme in Figure 2A). Of note, we tested various combinations of expression timing of *MyoD* and *BAF60C2* in different hESC lines and observed the activation of the myogenic program only when *BAF60C2* was expressed prior to *MyoD* (data not shown). This protocol led to a dramatic enhancement in the activation of the myogenic program in $hESC^{BAF60C2/MyoD}$, with the generation of a homogeneous population of committed cells (Figure 2B, pre-EB conditions) that became competent to activate skeletal myogenesis upon aggregation into EB-like clusters, leading to massive formation of myogenin/MyHC-positive myotubes after dissociation and exposure to DM conditions (Figures 2B [post-EB conditions] and 2C). Under these conditions, the percentage of myogenic conversion of $hESC^{BAF60C2/MyoD}$ was much higher (60.1% ± 5% MyHC-positive cells) (Figure 2B) than that observed in standard conditions for myogenic conversion shown in Figure 1D (4.67% ± 0.8% MyHC-positive cells). Sporadic formation of myogenin-positive cells was observed in MyoD-expressing H9 hESCs ($hESC^{MyoD}$) cultured in EB medium (Figures 2B and 2C), possibly due to localized upregulation of endogenous BAF60C2 or to the compensatory activity of BAF60B, as previously described for cardiomyogenesis (Takeuchi and Bruneau, 2009). However, only $hESC^{BAF60C2/MyoD}$ differentiated into MyHC-positive myotubes with high efficiency after culture in EB conditions (60.1% ± 5% MyHC-positive cells from $hESC^{BAF60C2/MyoD}$ versus 2.5% ± 0.5% from $hESC^{MyoD}$). Interestingly, forced expression of BAF60C2 alone in hESCs ($hESC^{BAF60C2}$) could not activate the skeletal myogenesis in the absence of MyoD (Figure 2B), indicating that BAF60C2 requires the presence of MyoD to activate muscle gene expression. These results indicate a multistep progression of $hESC^{BAF60C2/MyoD}$ through sequential stages of cellular differentiation, including lineage determination by MyoD and BAF60C2 (pre-EB stage) followed by competence to respond to differentiation signals and formation of terminally differentiated myotubes (post-EB stages). Previous works demonstrated the key role of BAF60C2 in at least two essential epigenetic events underlying myogenic differentiation, such as MyoD binding to the chromatin of target genes and the signal-dependent recruitment of BRG1-based SWI/SNF chromatin remodeling complex (Forcales et al., 2012). We used chromatin immunoprecipitation (ChIP) to investigate the sequential recruitment of MyoD, BAF60C2, and BRG1 to MyoD target genes in $hESC^{BAF60C2/MyoD}$ or $hESC^{MyoD}$ or control PGK-infected hESCs ($hESC^{Pgk}$) at pre-EB and post-EB stages. We focused on human *MYOGENIN* gene, since activation of *MYOGENIN* transcription is invariably required for the execution of the myogenic program during development and post-natal life (Hasty et al., 1993; Ohkawa et al., 2006). Moreover, the sequential recruitment of MyoD/BAF60C complex, followed by BRG1-based SWI/SNF complex, has been demonstrated on *myogenin* promoter in skeletal myoblasts (Forcales et al., 2012). In the absence of BAF60C2 ($hESC^{MyoD}$), MyoD could not bind the *MYOGENIN* promoter either in pre-EB conditions or after exposure to the differentiation signals within EB-like clusters (post-EB conditions) (Figure 2D). Forced expression of BAF60C2 ($hESC^{BAF60C2/MyoD}$) enabled MyoD recruitment to *MYOGENIN* promoter together with BAF60C2, but not BRG1, in pre-EB conditions (Figure 2D). Formaldehyde-assisted isolation of regulatory elements (FAIRE) showed that BAF60C2 and MyoD binding to MYOGENIN promoter correlated with incipient chromatin accessibility in correspondence of the PBX binding site (Berkes et al., 2004) in $hESC^{BAF60C2/MyoD}$ as compared to control lines in pre-EB conditions (Figure 2E). This evidence

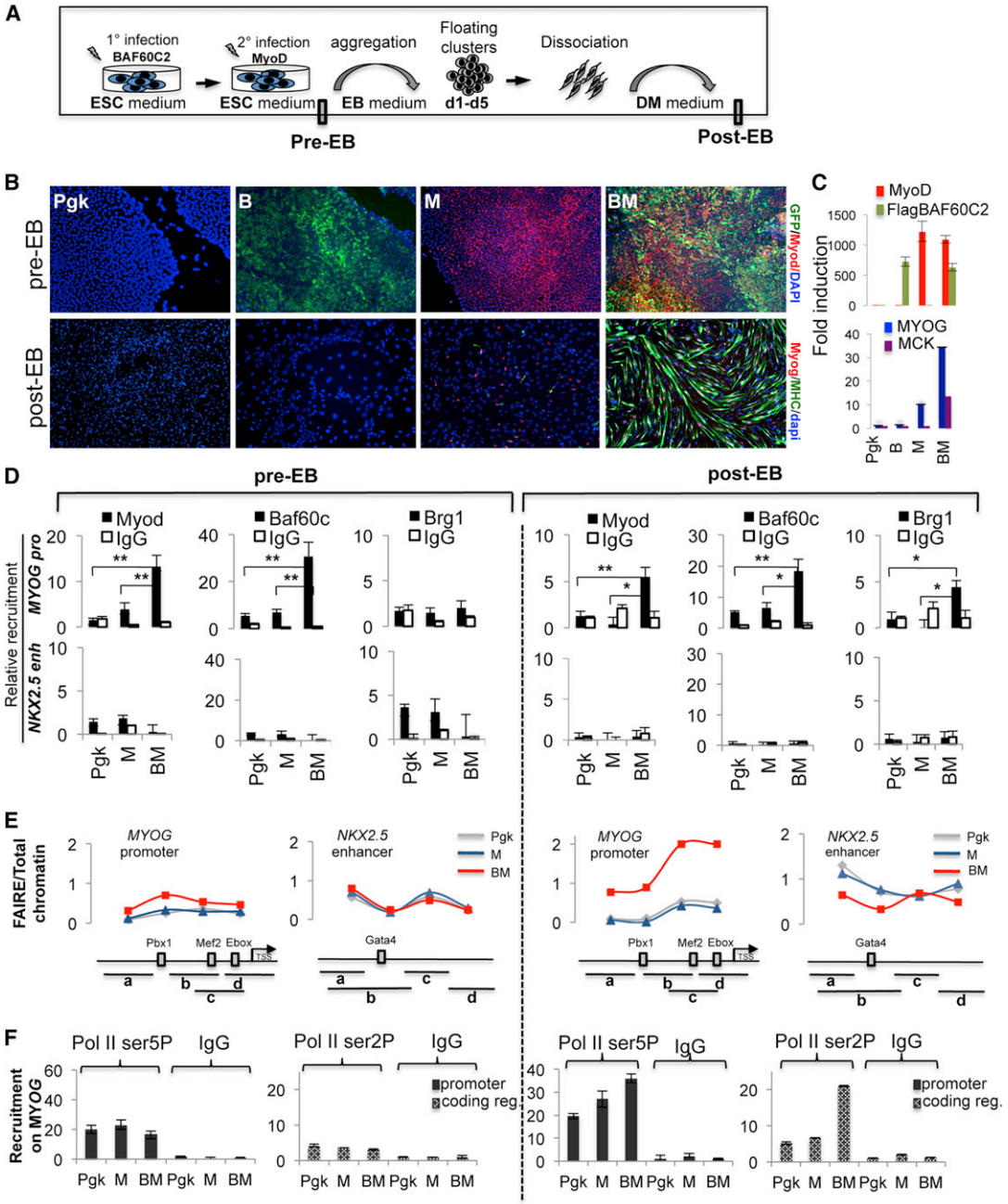

Figure 2. Efficient Generation of Muscle Cells from hESC$^{BAF60c2/MyoD}$ Is Achieved through BAF60C-Dependent Chromatin Targeting of MyoD prior to Differentiation into EBs

(A) Protocol to derive muscle cells from undifferentiated hESCs (H9) infected sequentially with BAF60C2 (B) and MyoD (M) lentiviruses. Cells were collected at the pre-EB or post-EB stages, as indicated, for further analysis.

(B) Representative images of hESCs infected with control (Pgk), BAF60C2-IRESGFP, MyoD, and BAF60C2/MyoD lentiviruses. Pre-EB cells were stained with antibodies against MyoD and green fluorescent protein to reveal exogenous proteins. Post-EB cells were stained for MHC and myogenin (Myog) to monitor the myogenic conversion.

(C) qRT-PCR analysis performed at pre- and post-EB stage. Error bars represent ±SD.

(D) ChIP analysis on *MYOGENIN* promoter and *NKX2.5* enhancer. Chromatin from Pgk, M, and BM cells at pre-EB and post-EB stages was immunoprecipitated with antibodies against MyoD, Baf60c, and Brg1, and IgG was used as a control. Protein recruitment is expressed as relative enrichment of each factor (black bars) compared to IgG (white bars) after normalization for total input control (n = 3; error bars represent SEM).

(E) FAIRE assay performed in pre- and post-EB cells to assess chromatin status on *MYOGENIN* promoter and *NKX2.5* enhancer. A representative experiment is shown (n = 3). Primer amplicons are depicted.

(F) Recruitment of Pol II ser5P and Pol II ser2P on *MYOGENIN* promoter or coding region performed on pre-EB and post-EB cells as described in (D).

indicates an instructive role of BAF60C2 in the early recognition of MyoD target sequences. Moreover, only in hESC$^{BAF60C2/MyoD}$ BRG1 recruitment to *MYOGENIN* promoter was detected in response to differentiation signals (post-EB conditions) (Figure 2D). The recruitment of BRG1-based SWI/SNF complex correlated with a dramatic enhancement in chromatin accessibility that was extended to the MEF2/Ebox sites (Figure 2E) and the engagement of the elongation-competent (serine 2 phosphorylated) form of polymerase II (Pol II ser2P) (Figure 2F), leading to activation of transcription (Figure 2C). Interestingly, serine 5 phosphorylated Pol II (Pol II ser5P) was detected at the transcription start site of *MYOGENIN* promoter in hESCs regardless the presence of MyoD and/or BAF60C2 (Figure 2F), according to the "poised" conformation of the chromatin at tissue-specific genes previously described in ESCs (Azuara et al., 2006; Boyer et al., 2006; Lee et al., 2006; Mikkelsen et al., 2007). Of note, BAF60C2 and BRG1 were not detected on the enhancer of the cardiac-specific gene *NKX2.5* in hESC$^{BAF60C2/MyoD}$ (Figure 2D). *NKX2.5* is induced by BAF60C2 and the transcriptional activators GATA4 and TBX5 in cardiac progenitors (Lickert et al., 2004; Takeuchi and Bruneau, 2009) and was expressed in control hESC^{Pgk} and hESC^{MyoD}, but not in hESC$^{BAF60C2/MyoD}$ (see Figure 3A). Consistently, *NKX2.5* enhancer showed a closed chromatin conformation in hESC$^{BAF60C2/MyoD}$, while in hESC^{Pgk} and hESC^{MyoD} an increased accessibility was detected at GATA4 binding sites (Figure 2E). This evidence further supports the conclusion that BAF60C2 enables selective activation of skeletal muscle genes by MyoD. The sequential and dynamic chromatin modifications shown in Figures 2D–2F define two distinct stages that reflect a "silent" epigenetic commitment to the myogenic lineage (pre-EB conditions) followed by the transcriptional activation of muscle genes in post-EB conditions.

Ectopic Expression of BAF60C2/MyoD Bypasses the Requirement for Mesodermal Transition to Promote Skeletal Myogenesis in hESCs

The direct activation of muscle gene expression by MyoD in hESC$^{BAF60C2/MyoD}$ is consistent with the nuclear reprogramming toward the skeletal muscle lineage, which is typically accompanied by the silencing of pluripotency genes and repressing alternative cell fates. Indeed, pluripotency genes were readily repressed in hESCs upon MyoD and BAF60C2 expression (data not shown), likely reflecting the functional antagonism between tissue-specific transcriptional activators and pluripotency. Similarly, markers of the alternative lineages within the three germ layers were repressed in hESC$^{BAF60C2/MyoD}$ as compared to hESC^{Pgk} (Figure 3A). Most of these markers showed a peak of expression between days 3 and 5 in hESC^{Pgk}-derived EBs but not in hESC$^{BAF60C2/MyoD}$-derived EBs (Figure 3A). Interestingly, while the expression pattern of many of these genes was partly overlapping in hESC^{MyoD}- and hESC$^{BAF60C2/MyoD}$-derived EB-like clusters during the first days of cultures in EB conditions, a late increase (between days 4 and 5) in the expression of lineage-specific markers, such as *NKX2.5, CERBERUS1*, and *NESTIN,* was observed in hESC^{MyoD}-derived aggregates (Figure 3A). This might reflect that ability of MyoD to repress pluripotency (Watanabe et al., 2011) via a BAF60C2-independent mechanism that leads to spontaneous commitment to various lineages by default (S.A. and P.L.P., unpublished data). Importantly, primitive markers of mesoderm (*BRACHYURY T, MESOGENIN*, and *MESP1)* were specifically repressed in hESC$^{BAF60C2/MyoD}$-derived EBs (Figure 3A). The only mesodermal gene that showed an earlier and more robust pattern of expression in hESC$^{BAF60C2/MyoD}$-derived EB-like clusters, as compared to hESC^{Pgk}- and hESC^{MyoD}-derived clusters, was the skeletal muscle progenitor marker *PAX3,* which establishes the myogenic identity within the paraxial mesoderm (Buckingham and Relaix, 2007) (Figure 3A). This is consistent with the selective activation of the skeletal muscle program in hESC$^{BAF60C2/MyoD}$. Figure 3B shows that hESC$^{BAF60C2/MyoD}$-derived EBs uniformly express PAX3 (78.5% ± 6%), while the primitive mesoderm marker BRACHYURY T could not be detected. By contrast, PAX3-positive cells were detected at much lower frequency in hESC^{Pgk}- and hESC^{MyoD}-derived EB-like clusters (10.0% ± 2.4% and 22.2% ± 3%, respectively), most of which coexpressed BRACHYURY T (Figure 3B), possibly reflecting the myogenic commitment of a subset of mesodermal derivatives. Thus, BAF60C2 and MyoD appear to generate an "epigenetic landscape" that imposes the selective activation of muscle gene expression in hESCs, leading to their direct conversion into skeletal myoblasts without the transition through the mesodermal stage. This evidence is well supported by the recruitment of BAF60C2 and BRG1 and activation of the *MYOGENIN* promoter, but not the *NKX2.5* enhancer, in hESC$^{BAF60C2/MyoD}$ (Figures 2D–2F).

To further demonstrate the homogeneous composition of hESC$^{BAF60C2/MyoD}$ by skeletal muscle progenitors, we dissociated hESC$^{BAF60C2/MyoD}$-derived EB-like clusters (as compared to the equivalent population from hESC^{Pgk} and hESC^{MyoD}) and sorted them by fluorescence-activated cell sorting (FACS) using the surface marker CD56 (NCAM1), which has previously been used to isolate human skeletal myoblasts (Zheng et al., 2007). Surprisingly, we found that the large majority of cells from dissociated hESC$^{BAF60C2/MyoD}$-derived floating aggregates, as well as hESC^{Pgk} and hESC^{MyoD}, were NCAM1 positive. This result reveals that NCAM1 expression cannot define by itself a population of skeletal muscle progenitors from hESCs and indicates that NCAM1 is probably expressed in cells undergoing transition toward a variety of lineages (Evseenko et al., 2010). However, when we measured the relative expression levels of NCAM1 in our hESC populations as compared to those of human primary skeletal myoblasts (HSkM), we found that hESC$^{BAF60C2/MyoD}$ were enriched in cells with expression levels (73%) of NCAM1 that were higher than those of hESC^{Pgk} (22%) and hESC^{MyoD} (54%) and similar to those detected in HSkM (data not shown). We therefore gated the high NCAM1-expressing cells among the population of NCAM1-positive FACS hESCs (Figure 3C) and measured their myogenic potential in vitro as percentage of myogenin/MyHC double-positive multinucleated cells formed among the same number of cells cultured in differentiation medium (Figure 3D). Figure 3D shows that the high NCAM-positive cells sorted from hESC$^{BAF60C2/MyoD}$-derived EB-like clusters evenly differentiated in myogenin/MYHC double-positive multinucleated myotubes (81.7% ± 3%), while only a minority of cells from hESC^{MyoD}-derived aggregates (4.3% ± 0.7%) and none of

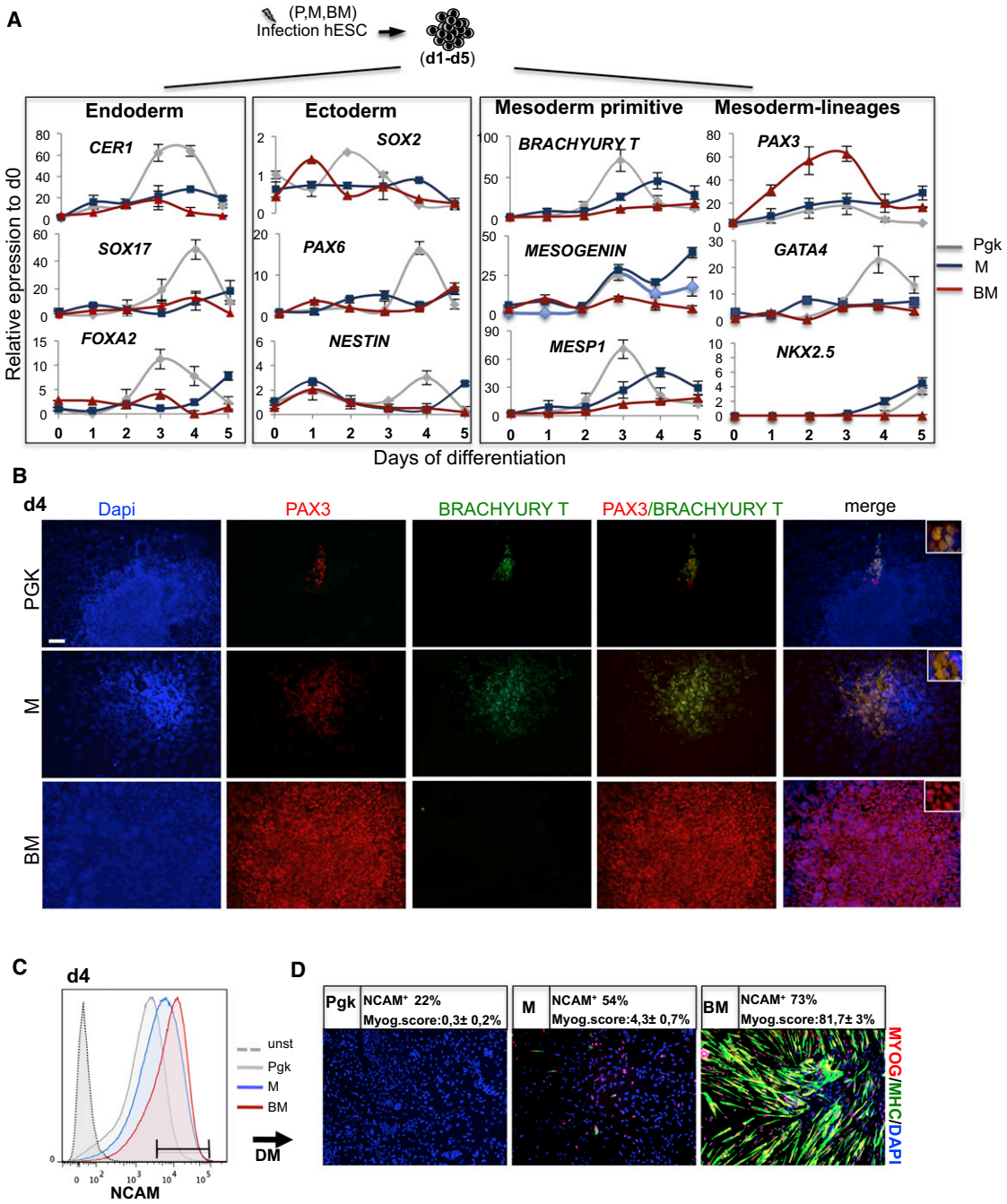

Figure 3. Direct Generation of Myogenic Progenitors from hESC$^{BAF60C2/MyoD}$

(A) hESCs H9 infected with control (Pgk), MyoD (M), or BAF60C2+MyoD (BM) were collected for 5 consecutive days from the onset of differentiation into EB-like clusters and analyzed by qRT-PCR to monitor the expression of genes indicative of the three germ layers (mesoderm, endoderm, ectoderm). Values are expressed as relative to Pgk day 0. Error bars represent SEM (n = 3).

(B) EB-like clusters at day 4 (d4) were stained for early precursor markers BRACHYURY T and PAX3. Scale bars are 50 μm. Insets show the higher magnification of nuclear staining for the indicated proteins.

(C and D) Isolation and characterization of CD56^{pos} (expressing high levels of CD56) population sorted from day 5 aggregates derived from hESCs infected with Pgk, MyoD, or BAF60C2/MyoD. Histogram plots show the specific staining signal (Pgk, M, BM) versus unstained signal (unst) and the percentage of cells expressing CD56 (NCAM) (C). CD56^{pos} cells were induced to differentiate and analyzed for the expression of skeletal muscle proteins myogenin and MHC by immunofluorescence (D).

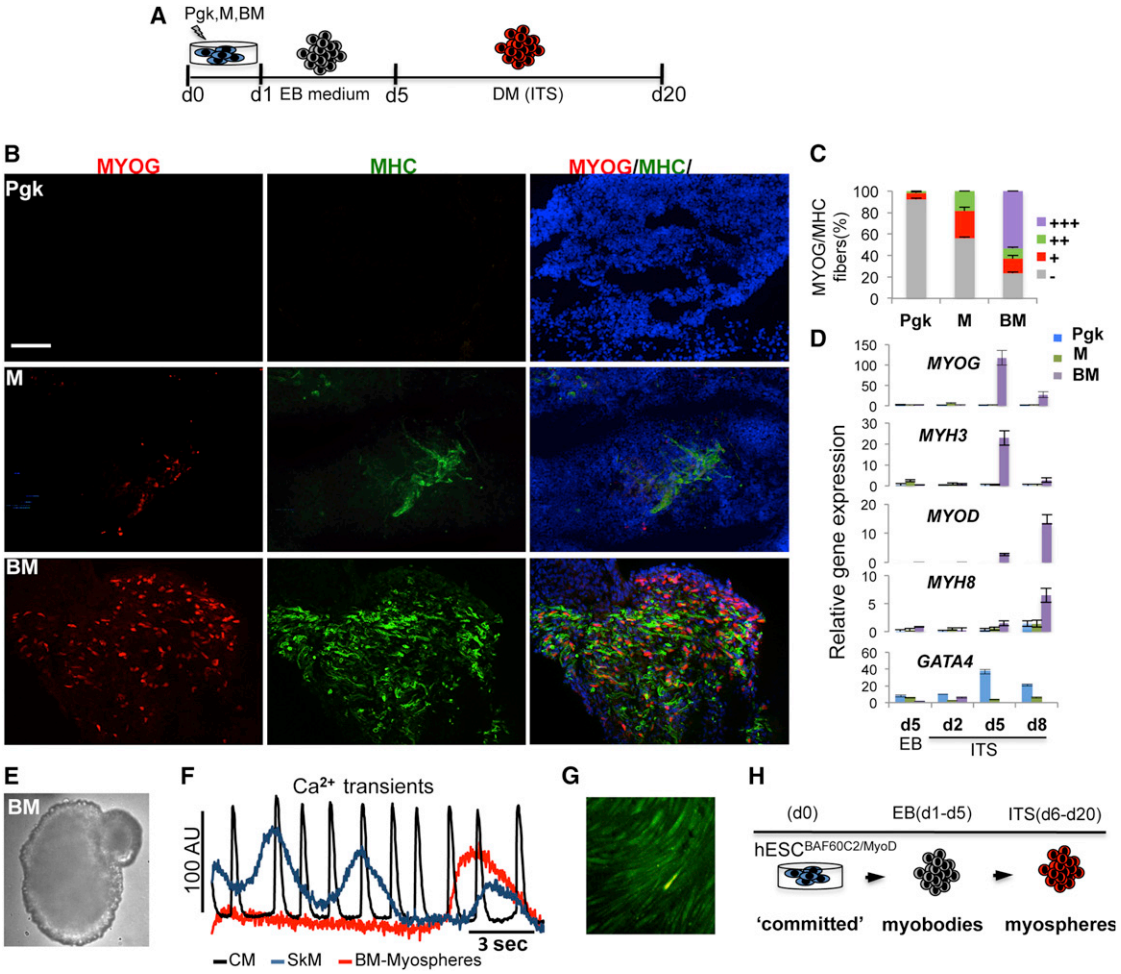

Figure 4. Generation of Skeletal Myospheres from hESC$^{BAF60C2/MyoD}$ and Electrophysiological Properties

(A) Schematic representation of the protocol used to generate 3D-skeletal myospheres.

(B) hESCs cultured in EB conditions to generate EBs according to the protocol depicted in (A) were subsequently sectioned and stained for the indicated muscle markers.

(C) Percentage of MYOG/MHC-positive cells within single EBs. EBs were classified based on the enrichment of myogenic fibers as follows: no myofibers (−), up to 10% (+), up to 30% (++), up to 100% (+++).

(D) Representative profile of gene expression of myogenic markers such as *MYOG,* embryonic MYHC (MYH3), perinatal MYHC (MYH8), *MYOD1*, and the cardiac marker *GATA4*. Values are expressed as relative to Pgk day 0 (bars represent SD).

(E) Snapshot from Movie S1 showing contraction of myospheres.

(F) Representative calcium transient recordings in hESC-derived cardiomyocytes (CM, black line), human skeletal myotubes derived from human fibroblasts converted by MyoD (SkM, blue line), and hESC$^{BAF60C2/MyoD}$-derived myospheres (red line).

(G) Snapshot from Movie S2 showing the local calcium distribution inside skeletal muscle cells.

(H) Scheme of the three-step generation of myospheres form hESC$^{BAF60C2/MyoD}$.

See also Figure S3.

the cells from hESC^{Pgk}-derived bodies could differentiate into myotubes under the same conditions. This result demonstrates that hESC$^{BAF60C2/MyoD}$-derived EB-like clusters are composed of a homogeneous population of skeletal myoblasts that retain the ability to differentiate into skeletal myotubes.

Generation of Contractile Myospheres from hESC$^{BAF60C2/MyoD}$

We therefore hypothesized that such a homogeneous population of hESC-derived myoblasts could bias the composition of EB-like clusters toward the formation of 3D contractile structures enriched in skeletal myofibers (skeletal myospheres). We devised a specific protocol by culturing hESC$^{BAF60C2/MyoD}$ (or hESC^{Pgk} and hESC^{MyoD}) in EB medium for 5 days, followed by the exposure of derived EB-like clusters to myogenic differentiation medium for additional 14 days (see scheme in Figure 4A). This protocol differs from the one shown in Figure 2A because it does not include dissociation of floating EB-like clusters and is therefore permissive for the formation of 3D structures. Only hESC$^{BAF60C2/MyoD}$ gave rise to EB-like structures that were fully

enriched in myogenin/MyHC-positive myofibers (Figures 4B and 4C) and expressed typical skeletal muscle markers, such as myogenin, MyH3, and MyH8, but not cardiac-specific genes, such as GATA4 (Figure 4D). hESC^{MyoD}-derived EBs showed rare areas, rather than diffuse formation, of myogenin/MYHC-positive cells (Figures 4B and 4C), possibly reflecting localized concentrations of EB-derived signals, such as morphogenes, that might induce endogenous BAF60C2 expression in MyoD-expressing cells. Importantly, hESC$^{BAF60C2/MyoD}$-derived EB-like structures underwent spontaneous contraction at very high frequency, as it was detected in about 20% of the EBs during 60 s observation of each plate (Movie S1 [snapshot in Figure 4E]; Figure S3A). We therefore defined them as contractile "myospheres." Dissociation of hESC$^{BAF60C2/MyoD}$-derived myospheres resulted in the formation of myogenin/MyHC-positive myofibers (Figure S3B). We investigated the contractile activity of hESC$^{BAF60c2/MyoD}$-derived myospheres. We used dynamic distribution of the cytosolic calcium in live cells to discriminate skeletal muscle-type contraction from cardiac-type contraction behavior. Figure 4F and Movie S2 (snapshot in Figure 4G) show that hESC$^{BAF60c2/MyoD}$-derived myospheres are exhibiting the slow-rising long-lasting increase in local calcium concentration typical of skeletal muscle-type calcium artifacts (Capes et al., 2011). Individual fluorescent Fluo-4 signals from either intact myospheres derived from hESC$^{BAF60C2/MyoD}$ or dissociated cells from myospheres during 20 s recordings show intracellular calcium dynamics typically reflecting skeletal muscle contractions (Figure 4F, compare blue and red lines) that are clearly distinguished from cardiac contraction contractions (Figure 4F, black line; see also Movie S2). The finding that hESC$^{BAF60C2/MyoD}$-derived myospheres, either intact or dissociated, showed a pattern of calcium transient similar to control skeletal myotubes demonstrates that the vast majority of contracting cells in hESC$^{BAF60c2/MyoD}$-derived myospheres exhibit skeletal muscle contractile activity (Figures 4F and 4G). This evidence, together with the lack of activation (Figure 2) and expression (Figures 3 and 4) of cardiac markers, conclusively demonstrates that BAF60C2 and MyoD are sufficient to convert hESCs into a homogeneous population of committed myoblasts that, when cultured in EB conditions, generate 3D contractile myospheres. These data emphasize the importance of imposing an epigenetic landscape that commits hESCs to myogenic progenitors and makes them competent to respond to the signals derived from EB-like structures (myobodies), ultimately leading to the formation of spontaneously contracting myospheres (Figure 4H).

Collectively, these data demonstrate that the requirement for transition through the mesodermal stage to activate myogenesis in hESCs can be bypassed by forced expression of BAF60C2 and MyoD. The identification of BAF60C2 as a limiting factor for the epigenetic reprogramming of hESCs to the myogenic lineage is of particular relevance because it provides the molecular explanation of the previously reported requirement of mesodermal transition to activate skeletal myogenesis in ESCs (Darabi et al., 2008, 2012; Iacovino et al., 2011). The evidence that BAF60C2 instructs tissue-specific transcriptional activators (such as MyoD) to activate lineage-specific gene expression suggests that repression of *BAF60C2* in undifferentiated hESCs is a necessary event to maintain pluripotency, presumably to prevent the formation of an epigenetic landscape permissive for commitment to the myogenic lineage. Along this line, we speculate that BAF60C2 derepression in hEBs (mimicked in our experimental conditions by hESC$^{BAF60c2/MyoD}$) might confer on hESCs the competence to properly respond to complex intracellular events elicited by external signals (e.g., activation of p38 and AKT pathways) (Serra et al., 2007) and developmental cues, such as TGFbeta-SMAD2/3 signaling (Capes et al., 2011) that enable MyoD to activate muscle gene expression. Overall, the ability to epigenetically reprogram hESCs into a homogenous population of skeletal muscle progenitors that can generate 3D contractile myospheres provides an unprecedented opportunity to establish "in dish" models of study of skeletal muscle physiology and mechanism of diseases.

EXPERIMENTAL PROCEDURES

hESC Culture

Undifferentiated hESCs, H9 and H1 (passages 35–45), were cultured and manipulated as indicated in Extended Experimental Procedures.

Intracellular Calcium Recording Assays in Living Cells

Calcium-transient hESC cell clusters were recorded using the IC100 High Content Imaging system equipped with the KIC (Kinetic Image Cytometer) electrical field stimulation module. For labeling and recording, see Extended Experimental Procedures.

Immunofluorescence and Immunocytochemical Analysis

See Extended Experimental Procedures for the details and antibody used. EBs were prepared according the protocol described in Gomes et al. (2010).

Gene Expression Analysis

Total RNA was isolated with TRIzol and retrotranscribed using reverse transcription reagent (Applied Biosystems). qRT-PCR was performed according the manufacturer's instructions on Mx3000P (Stratagene) using SYBR Green Master Mix. Data were normalized to the expression of GAPDH gene (for SYBR Green) and relative quantification was calculated by the Comparative Ct method. Primers used are listed in Table S1.

FAIRE

Chromatin for FAIRE (formaldehyde-assisted isolation of regulatory elements) analysis was prepared as previously described in Simon et al. (2012). A total of 10 ng of FAIRE purified DNA or 10 ng of purified input DNA was analyzed by qRT-PCR. The signal of FAIRE-purified chromatin is presented as a fraction of input-purified chromatin. See details in Extended Experimental Procedures. Primers used are listed in Table S1.

ChIP Assay

ChIP was performed as described in Forcales et al. (2012) with some modifications (see Extended Experimental Procedures for details). Chromatin extracts were immunoprecipitated overnight on rotating platform at 4°C with the following antibodies: anti-MyoD (Santa Cruz, sc-760) anti-Brg1 (Santa Cruz, sc-17796X), custom-made anti-BAF60c antibody, anti-Pol II ser5P (39233, active motif) and anti-Pol II ser2P (Abcam, ab24758) with immunoglobulin (Ig) G-IgM linker antibody (Abcam, ab9175) or normal IgG as control. Primers used are listed in Table S1.

Statistical Analysis

Data are presented as mean ± SEM unless otherwise indicated. Differences between groups were analyzed for statistical significance using unpaired the Student's t test with significance being defined as $*p < 0.05$, $**p < 0.01$, or $***p < 0.001$.

SUPPLEMENTAL INFORMATION

Supplemental Information includes Extended Experimental Procedures, three figures, one table, and two movies and can be found with this article online at http://dx.doi.org/10.1016/j.celrep.2013.02.012.

LICENSING INFORMATION

ACKNOWLEDGMENTS

P.L.P. is an Associate Investigator of Sanford Children's Health Research Center. This work was supported by the following grants (to P.L.P.): R01AR056712, R01AR052779, and P30 AR061303 from the National Institutes of Health/National Institute of Arthritis and Musculoskeletal and Skin Diseases, MDA, and Sanford Children Health Research award. This work partly benefited from research funding from the European Community's Seventh Framework Programme in the project FP7-Health – 2009 ENDOSTEM 241440 (Activation of vasculature associated stem cells and muscle stem cells for the repair and maintenance of muscle tissue). S.A. was supported by a CIRM fellowship.

S.A. performed most of the experiments with the help of P.C.; L.G. performed FACS on NCAM1-positive hESCs; B.M. performed the FAIRE assay; and A.S. performed the assay of intracellular calcium recording in living cells. S.F. provided the evidence that BAF60 was necessary for MyoD-mediated activation of gene expression in embryonic stem cells. P.L.P. conceived the project and the experiments, analyzed the data, and wrote the manuscript. All authors discussed and commented on the results and read the manuscript. We thank Natalie Prigozhina for help with EB recording.

Received: October 10, 2012
Revised: December 27, 2012
Accepted: February 6, 2013
Published: March 7, 2013

REFERENCES

Azuara, V., Perry, P., Sauer, S., Spivakov, M., Jørgensen, H.F., John, R.M., Gouti, M., Casanova, M., Warnes, G., Merkenschlager, M., and Fisher, A.G. (2006). Chromatin signatures of pluripotent cell lines. Nat. Cell Biol. *8*, 532–538.

Barberi, T., Bradbury, M., Dincer, Z., Panagiotakos, G., Socci, N.D., and Studer, L. (2007). Derivation of engraftable skeletal myoblasts from human embryonic stem cells. Nat. Med. *13*, 642–648.

Berkes, C.A., Bergstrom, D.A., Penn, B.H., Seaver, K.J., Knoepfler, P.S., and Tapscott, S.J. (2004). Pbx marks genes for activation by MyoD indicating a role for a homeodomain protein in establishing myogenic potential. Mol. Cell *14*, 465–477.

Boyer, L.A., Plath, K., Zeitlinger, J., Brambrink, T., Medeiros, L.A., Lee, T.I., Levine, S.S., Wernig, M., Tajonar, A., Ray, M.K., et al. (2006). Polycomb complexes repress developmental regulators in murine embryonic stem cells. Nature *441*, 349–353.

Buckingham, M., and Relaix, F. (2007). The role of Pax genes in the development of tissues and organs: Pax3 and Pax7 regulate muscle progenitor cell functions. Annu. Rev. Cell Dev. Biol. *23*, 645–673.

Capes, E.M., Loaiza, R., and Valdivia, H.H. (2011). Ryanodine receptors. Skelet. Muscle *1*, 18.

Chambers, S.M., and Studer, L. (2011). Cell fate plug and play: direct reprogramming and induced pluripotency. Cell *145*, 827–830.

Darabi, R., Gehlbach, K., Bachoo, R.M., Kamath, S., Osawa, M., Kamm, K.E., Kyba, M., and Perlingeiro, R.C. (2008). Functional skeletal muscle regeneration from differentiating embryonic stem cells. Nat. Med. *14*, 134–143.

Darabi, R., Arpke, R.W., Irion, S., Dimos, J.T., Grskovic, M., Kyba, M., and Perlingeiro, R.C. (2012). Human ES- and iPS-derived myogenic progenitors restore DYSTROPHIN and improve contractility upon transplantation in dystrophic mice. Cell Stem Cell *10*, 610–619.

de la Serna, I.L., Ohkawa, Y., and Imbalzano, A.N. (2006). Chromatin remodelling in mammalian differentiation: lessons from ATP-dependent remodellers. Nat. Rev. Genet. *7*, 461–473.

Debril, M.B., Gelman, L., Fayard, E., Annicotte, J.S., Rocchi, S., and Auwerx, J. (2004). Transcription factors and nuclear receptors interact with the SWI/SNF complex through the BAF60c subunit. J. Biol. Chem. *279*, 16677–16686.

Evseenko, D., Zhu, Y., Schenke-Layland, K., Kuo, J., Latour, B., Ge, S., Scholes, J., Dravid, G., Li, X., MacLellan, W.R., and Crooks, G.M. (2010). Mapping the first stages of mesoderm commitment during differentiation of human embryonic stem cells. Proc. Natl. Acad. Sci. USA *107*, 13742–13747.

Forcales, S.V., Albini, S., Giordani, L., Malecova, B., Cignolo, L., Chernov, A., Coutinho, P., Saccone, V., Consalvi, S., Williams, R., et al. (2012). Signal-dependent incorporation of MyoD-BAF60c into Brg1-based SWI/SNF chromatin-remodelling complex. EMBO J. *31*, 301–316.

Gerber, A.N., Klesert, T.R., Bergstrom, D.A., and Tapscott, S.J. (1997). Two domains of MyoD mediate transcriptional activation of genes in repressive chromatin: a mechanism for lineage determination in myogenesis. Genes Dev. *11*, 436–450.

Gomes, I.C., Acquarone, M., Maciel Rde, M., Erlich, R.B., and Rehen, S.K. (2010). Analysis of pluripotent stem cells by using cryosections of embryoid bodies. J. Vis. Exp. *46*, 2344. http://dx.doi.org/10.3791/2344.

Goudenege, S., Lebel, C., Huot, N.B., Dufour, C., Fujii, I., Gekas, J., Rousseau, J., and Tremblay, J.P. (2012). Myoblasts derived from normal hESCs and dystrophic hiPSCs efficiently fuse with existing muscle fibers following transplantation. Mol. Ther. *20*, 2153–2167.

Guasconi, V., and Puri, P.L. (2009). Chromatin: the interface between extrinsic cues and the epigenetic regulation of muscle regeneration. Trends Cell Biol. *19*, 286–294.

Hasty, P., Bradley, A., Morris, J.H., Edmondson, D.G., Venuti, J.M., Olson, E.N., and Klein, W.H. (1993). Muscle deficiency and neonatal death in mice with a targeted mutation in the myogenin gene. Nature *364*, 501–506.

Ho, L., Ronan, J.L., Wu, J., Staahl, B.T., Chen, L., Kuo, A., Lessard, J., Nesvizhskii, A.I., Ranish, J., and Crabtree, G.R. (2009). An embryonic stem cell chromatin remodeling complex, esBAF, is essential for embryonic stem cell self-renewal and pluripotency. Proc. Natl. Acad. Sci. USA *106*, 5181–5186.

Iacovino, M., Bosnakovski, D., Fey, H., Rux, D., Bajwa, G., Mahen, E., Mitanoska, A., Xu, Z., and Kyba, M. (2011). Inducible cassette exchange: a rapid and efficient system enabling conditional gene expression in embryonic stem and primary cells. Stem Cells *29*, 1580–1588.

Keller, G.M. (1995). In vitro differentiation of embryonic stem cells. Curr. Opin. Cell Biol. *7*, 862–869.

Krauss, R.S. (2010). Regulation of promyogenic signal transduction by cell-cell contact and adhesion. Exp. Cell Res. *316*, 3042–3049.

Lee, T.I., Jenner, R.G., Boyer, L.A., Guenther, M.G., Levine, S.S., Kumar, R.M., Chevalier, B., Johnstone, S.E., Cole, M.F., Isono, K., et al. (2006). Control of developmental regulators by Polycomb in human embryonic stem cells. Cell *125*, 301–313.

Lickert, H., Takeuchi, J.K., Von Both, I., Walls, J.R., McAuliffe, F., Adamson, S.L., Henkelman, R.M., Wrana, J.L., Rossant, J., and Bruneau, B.G. (2004). Baf60c is essential for function of BAF chromatin remodelling complexes in heart development. Nature *432*, 107–112.

Mikkelsen, T.S., Ku, M., Jaffe, D.B., Issac, B., Lieberman, E., Giannoukos, G., Alvarez, P., Brockman, W., Kim, T.K., Koche, R.P., et al. (2007). Genome-wide maps of chromatin state in pluripotent and lineage-committed cells. Nature *448*, 553–560.

Ohkawa, Y., Marfella, C.G., and Imbalzano, A.N. (2006). Skeletal muscle specification by myogenin and Mef2D via the SWI/SNF ATPase Brg1. EMBO J. *25*, 490–501.

Reyes, J.C., Barra, J., Muchardt, C., Camus, A., Babinet, C., and Yaniv, M. (1998). Altered control of cellular proliferation in the absence of mammalian brahma (SNF2alpha). EMBO J. *17*, 6979–6991.

Sartorelli, V., and Juan, A.H. (2011). Sculpting chromatin beyond the double helix: epigenetic control of skeletal myogenesis. Curr. Top. Dev. Biol. *96*, 57–83.

Takeuchi, J.K., and Bruneau, B.G. (2009). Directed transdifferentiation of mouse mesoderm to heart tissue by defined factors. Nature *459*, 708–711.

Serra, C., Palacios, D., Mozzetta, C., Forcales, S.V., Morantte, I., Ripani, M., Jones, D.R., Du, K., Jhala, U.S., Simone, C., and Puri, P.L. (2007). Functional interdependence at the chromatin level between the MKK6/p38 and IGF1/PI3K/AKT pathways during muscle differentiation. Mol. Cell *28*, 200–213.

Simon, J.M., Giresi, P.G., Davis, I.J., and Lieb, J.D. (2012). Using formaldehyde-assisted isolation of regulatory elements (FAIRE) to isolate active regulatory DNA. Nat. Protoc. *7*, 256–267.

Wang, W., Xue, Y., Zhou, S., Kuo, A., Cairns, B.R., and Crabtree, G.R. (1996). Diversity and specialization of mammalian SWI/SNF complexes. Genes Dev. *10*, 2117–2130.

Watanabe, S., Hirai, H., Asakura, Y., Tastad, C., Verma, M., Keller, C., Dutton, J.R., and Asakura, A. (2011). MyoD gene suppression by Oct4 is required for reprogramming in myoblasts to produce induced pluripotent stem cells. Stem Cells *29*, 505–516.

Weintraub, H., Tapscott, S.J., Davis, R.L., Thayer, M.J., Adam, M.A., Lassar, A.B., and Miller, A.D. (1989). Activation of muscle-specific genes in pigment, nerve, fat, liver, and fibroblast cell lines by forced expression of MyoD. Proc. Natl. Acad. Sci. USA *86*, 5434–5438.

Zheng, B., Cao, B., Crisan, M., Sun, B., Li, G., Logar, A., Yap, S., Pollett, J.B., Drowley, L., Cassino, T., et al. (2007). Prospective identification of myogenic endothelial cells in human skeletal muscle. Nat. Biotechnol. *25*, 1025–1034.